Unveiling the Genomic Landscape of Intraductal Carcinoma of the Prostate Using Spatial Gene Expression Analysis

Ryuta Watanabe * , Noriyoshi Miura , Mie Kurata , Riko Kitazawa , Tadahiko Kikugawa , Takashi Saika

Posted Date: 18 March 2024

doi: 10.20944/preprints202403.1037.v1

Keywords: spatial gene expression analysis; intraductal carcinoma of the prostate (IDCP); hypoxic markers; immune cells; tumor microenvironment

Article

Unveiling the Genomic Landscape of Intraductal Carcinoma of the Prostate Using Spatial Gene Expression Analysis

Ryuta Watanabe [1,2,*], Noriyoshi Miura [1], Mie Kurata [3,4], Riko Kitazawa [5], Tadahiko Kikugawa [1] and Takashi Saika [1]

[1] Department of Urology, Ehime University Graduate School of Medicine, Ehime, Japan
[2] Human Biology Division, Fred Hutchinson Cancer Center, Seattle, Japan
[3] Department of Analytical Pathology, Ehime University Graduate School of Medicine, Ehime, Japan
[4] Division of Pathology, Proteo-Science Center, Ehime University, Ehime, Japan
[5] Division of Diagnostic Pathology, Ehime University Hospital, Ehime, Japan
* Correspondence: watanabe.ryuta.cu@ehime-u.ac.jp; Tel.: +81-89-960-5356, Fax: +81-89-960-5358

Abstract: Recently intraductal carcinoma of the prostate (IDCP) has attracted increasing interest owing to its unfavorable prognoses. To effectively identify the IDCP-specific gene expression profile, we took a novel approach of characterizing a typical IDCP case using spatial gene expression analysis. A formalin-fixed, paraffin-embedded sample was subjected to Visium CytAssist Spatial Gene Expression analysis. IDCP within invasive prostate cancer sites was recognized as a distinct cluster separate from other invasive cancer clusters. Highly expressed genes defining the IDCP cluster, such as *MUC6*, *MYO16*, *NPY*, and *KLK12*, reflected the aggressive nature of high-grade prostate cancer. IDCP sites also showed increased hypoxia markers *HIF1A*, *BNIP3L*, *PDK1*, and *POGLUT1*; decreased fibroblast markers *COL1A2*, *DCN*, and *LUM*; and decreased immune cell markers *CCR5* and *FCGR3A*. Overall, these findings indicate that the hypoxic tumor microenvironment and reduced accessibility to immune cells, which reflect the pathological characteristics of IDCP, may influence the aggressiveness of high-grade prostate cancer.

Keywords: spatial gene expression analysis; intraductal carcinoma of the prostate (IDCP); hypoxic markers; immune cells; tumor microenvironment

1. Introduction

Intraductal carcinoma of the prostate (IDCP) is a condition in which atypical cells from outside the glandular ducts invade and proliferate in normal glandular structures, leaving behind some basal cells and showing a cribriform morphology and extensive growth pattern. In 1996, McNeal et al. first reported IDCP with invasive cancer [1]. Since then, IDCP has received increasing attention because of its association with poor prognosis. The presence of IDCP during radical prostatectomy has been reported to be associated with a higher Gleason score, larger tumor volume, extraprostatic extension, squamous cell carcinoma at the resection margin, and accelerated disease progression [2–5]. Further, patients with localized and advanced prostate cancer (PCa) with IDCP have been reported to show significantly worse recurrence-free and overall survival rates [6–9].

For these reasons, IDCP was first described by the International Society of Urologic Pathology in 2014 [10] and subsequently included in the 2016 World Health Organization Prostate Tumor Classification [11], 2017 American Society of Pathology guidelines, and 2019 National Comprehensive Cancer Network (NCCN) guidelines [12].

Reports from Western countries have shown that homologous recombination (HR) gene mutations, including *BRCA* mutations, in addition to *TMPRSS2-ERG* fusion gene and *TP53*, *RB1*, and *PTEN* deletions, are frequently detected in patients with IDCP [13–16]. Interestingly, one study

 doi:10.20944/preprints202403.1037.v1

reported the presence of *BRCA2* mutations in approximately 42% of IDCP cases [17,18]; further, the NCCN guidelines state that early genetic testing should be considered in prostate cancer patients with IDCP. Therefore, identifying IDCP-specific genetic abnormalities will contribute to the elucidation of molecular mechanisms underlying IDCP pathogenesis and the promotion of precision medicine.

Prostate cancer is extremely heterogeneous; therefore, gene expression analysis specific to IDCP lesions using conventional bulk gene analysis is impossible. Single-cell RNA-seq allows an understanding of tumor heterogeneity based on gene expression at the single-cell level. However, as IDCP is a morphology-based diagnosis, application of single-cell RNA-seq is unsuitable because of the loss of spatial information. Therefore, in this study, we made a groundbreaking attempt to analyze the gene abnormalities characteristic of IDCP sites while maintaining the spatial information of IDCP using spatial gene expression analysis technology.

2. Materials and Methods

2.1. IDCP Diagnosis

We retrospectively reviewed patients who underwent total prostatectomy for PCa at Ehime University Hospital and selected suspected IDCP cases. For these patients, immunohistochemistry was performed on 10% neutral buffered formalin-fixed and paraffin-embedded surgical tissue samples, which were sectioned on a microtome (3–5 μm thick) and stained according to standard protocols. An anti-basal cell antibody (p63 antibody + HMW cytokeratin antibody) purchased from Proteintech (US) was used to stain the basal cells, and Hoechst 33342 (dilution 1:2000; Molecular Probes) was used to stain the nuclei.

Three pathologists from Ehime University Hospital, including a skilled U.S pathologist specializing in IDCP diagnosis, reviewed the pathology reports to identify cases suggestive of IDCP and to determine the presence of IDCP indicators. Finally, one case was used for the study.

This study was approved by the Institutional Review Board of Ehime University (Nos. 2108006, 2109014, and 2205001) and was conducted according to the principles of the Declaration of Helsinki. Written informed consent was obtained from the patient for publication of the case report and accompanying images.

2.2. Spatial Transcriptomics (CytAssist Visium)

Spatial transcriptomics analyses were performed as previously described (Watanabe et al. 2023) [19]. Formalin-fixed, paraffin-embedded (FFPE) samples that passed the RNA quality control (DV200 > 50%) were used for spatial transcriptomic construction and sequencing. The tissues were prepared according to the Visium CytAssist Spatial Gene Expression for FFPE-Tissue Preparation Guide (CG000518, 10x Genomics, CA, USA). Sequencing was performed at the Research Institute for Microbial Diseases, Osaka University. Libraries were sequenced using an MGI DNBSEQ-G400RS (MGI Tech Co., SZX, CN). The Space Ranger pipeline v2022.0705.1 (10x Genomics, CA, USA) and the GRCh38-2020-A reference were used to process FASTQ files. The sequencing results were guaranteed to be accurate as follows.

Number of reads: 366,120,606; number of spots under tissue: 4,763; median genes per spot: 5,665; mean number of reads under tissue per spot: 70,197.

t-SNE plots and violin plots were run and plotted using the Loupe Browser (10x genomics, CA, USA). Trajectory and pathway enrichment analyses were performed and plotted using Partek flow software (Partek Incorporated, MO, USA).

3. Results

3.1. Diagnosis of IDCP and Clustering by Spatial Gene Expression Analysis

A 62-year-old man diagnosed with prostate adenocarcinoma (cT3aN0M0, high risk, PSA 31.5 ng/mL), underwent a robot-assisted laparoscopic prostatectomy. Basal cell staining was performed

 doi:10.20944/preprints202403.1037.v1

on FFPE slides of total prostatectomy specimens with a Gleason score 4+5 prostate cancer background. Cribriform morphological growth of the tumor was evident in the normal glandular ducts with preserved basal cells, leading to a diagnosis of IDCP (Figure 1A,B). Spatial gene expression analysis (CytAssist Visium) categorized the prostate tissue cells into 10 clusters, with cluster 10 identified as an independent cluster corresponding to the IDCP region (Figure 1C,D). Clusters of invasive cancer lesions proximal to IDCP on the pathology slides exhibited gene expression patterns similar to those of the IDCP clusters on the t-SNE plot, whereas distant clusters showed distinct patterns (Figure 1E,F). Trajectory analysis further confirmed the lineage similarity between IDCPs and the neighboring invasive carcinomas (Figure 1G).

The 20 most highly expressed genes in the IDCP (cluster 10) and non-IDCP regions (Clusters 1-9) are shown in Figure 1F. Notably, *MUC6*, *MYO16*, *NPY*, and *KLK12* emerged as highly expressed genes defining the IDCP clusters, in contrast to genes from the tumor microenvironment, such as *LTF*, *MMP*, *ELN*, and *COL3A1*, which were relatively highly expressed in the non-IDCP clusters (Figure 1H). The volcano plot illustrates highly expressed genes in the IDCP and non-IDCP regions (Figure 1I). Additionally, heat maps underscored the differences in gene expression between the IDCP and non-IDCP regions (Figure 1J).

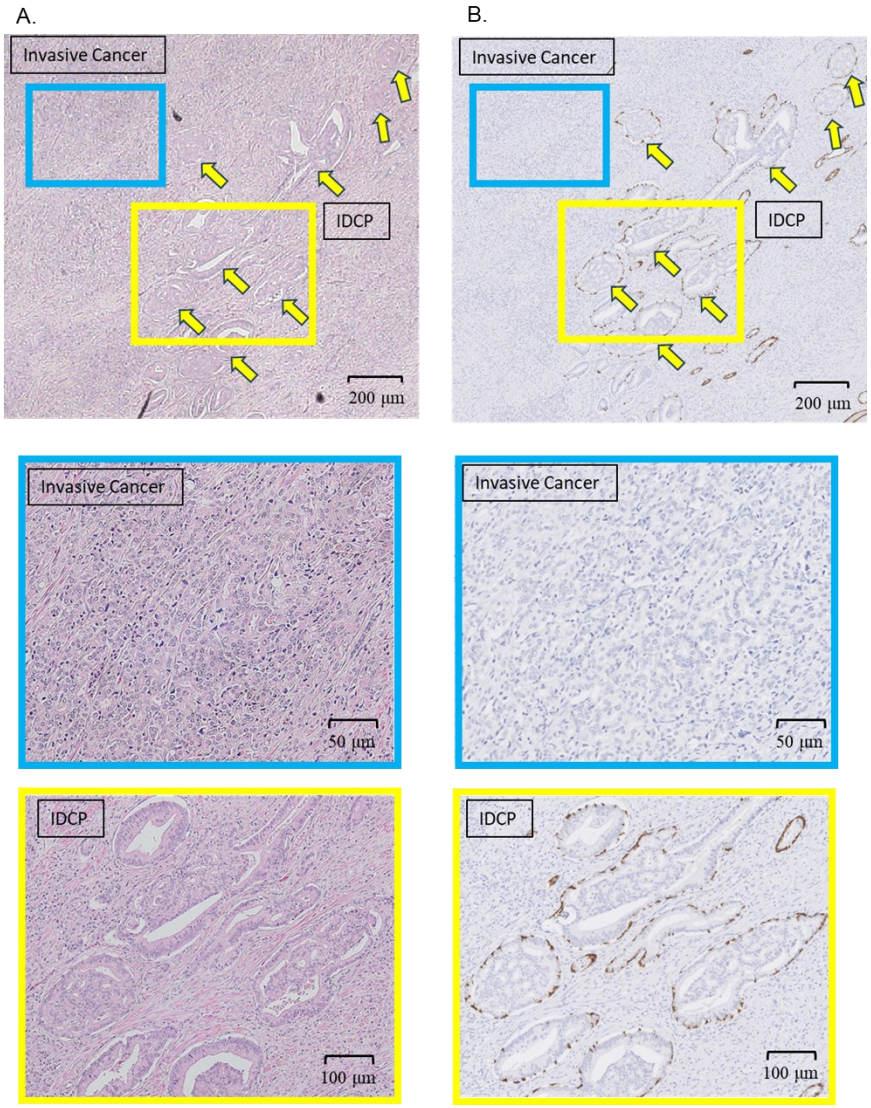

 doi:10.20944/preprints202403.1037.v1

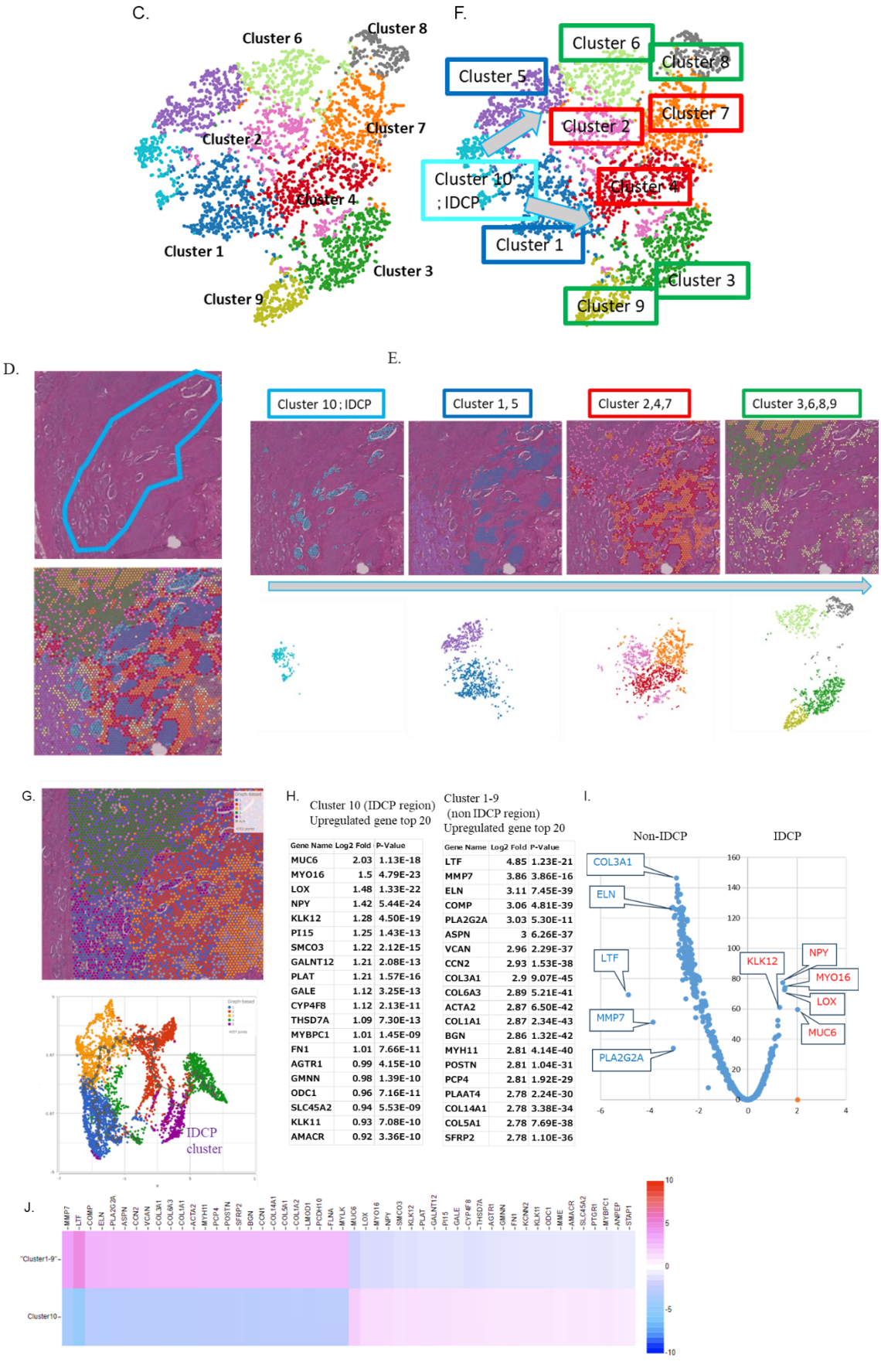

Gene Name	Log2 Fold	P-Value
MUC6	2.03	1.13E-18
MYO16	1.5	4.79E-23
LOX	1.48	1.33E-22
NPY	1.42	5.44E-24
KLK12	1.28	4.50E-19
PI15	1.25	1.43E-13
SMCO3	1.22	2.12E-15
GALNT12	1.21	2.08E-13
PLAT	1.21	1.57E-16
GALE	1.12	3.25E-13
CYP4F8	1.12	2.13E-11
THSD7A	1.09	7.30E-13
MYBPC1	1.01	1.45E-09
FN1	1.01	7.66E-11
AGTR1	0.99	4.15E-10
GMNN	0.98	1.39E-10
ODC1	0.96	7.16E-11
SLC45A2	0.94	5.53E-09
KLK11	0.93	7.08E-10
AMACR	0.92	3.36E-10

Gene Name	Log2 Fold	P-Value
LTF	4.85	1.23E-21
MMP7	3.86	3.86E-16
ELN	3.11	7.45E-39
COMP	3.06	4.81E-39
PLA2G2A	3.03	5.30E-11
ASPN	3	6.26E-37
VCAN	2.96	2.29E-37
CCN2	2.93	1.53E-38
COL3A1	2.9	9.07E-45
COL6A3	2.89	5.21E-41
ACTA2	2.87	6.50E-42
COL1A1	2.87	2.34E-43
BGN	2.86	1.32E-42
MYH11	2.81	4.14E-40
POSTN	2.81	1.04E-31
PCP4	2.81	1.92E-29
PLAAT4	2.78	2.24E-30
COL14A1	2.78	3.38E-34
COL5A1	2.78	7.69E-38
SFRP2	2.78	1.10E-36

Figure 1. Diagnosis of IDCP and clustering by spatial gene expression analysis. (**A**) A 62-year-old man diagnosed with prostate adenocarcinoma (cT3aN0M0, high risk, PSA 31.5 ng/mL), underwent a robot-assisted laparoscopic prostatectomy. HE staining reveals tumor invasion within normal glandular

 doi:10.20944/preprints202403.1037.v1

ducts with surrounding invasive carcinoma (blue square; invasive cancer area, yellow square; IDCP area, yellow arrow; IDCP). (**B**) Basal cell staining was performed on a formalin-fixed paraffin-embedded slide of the total prostatectomy specimen with a prostate cancer background showing Gleason Score 4+5. Cribriform morphological growth of the tumor was found in the normal glandular ducts with preserved basal cells, and IDCP was diagnosed (blue square; invasive cancer area, yellow square; IDCP area, yellow arrow; IDCP). (**C**, **D**) Spatial gene expression analysis (CytAssist Visium) classifies the cells of the prostate tissue into 10 clusters. Of these 10 clusters, cluster 19 matches the IDCP region. (**E**, **F**) The clusters of invasive cancer lesions outside normal glandular ducts that were close to those of IDCP on the pathology slides and were also close to IDCP clusters on the t-SNE plot, suggesting a similar gene expression pattern. (**G**) Trajectory analysis showed that IDCPs were similar in lineage to the neighboring invasive carcinomas. (**H**) The 20 most highly expressed genes in the IDCP (Cluster 10) and non-IDCP regions (Cluster 1-9). (**I**) The volcano plot shows the highly expressed genes in the IDCP and non-IDCP regions H) Heat maps showed differences in gene expression between the IDCP and non-IDCP regions. (**J**) Heatmap illustrates a clear distinction between gene expression in IDCP regions (cluster 10) and non-IDCP regions (clusters 1-9).

3.2. Visualization of Epithelial Cell, Androgen Receptor (AR) Signature Gene,and Other Upregulated Gene Marker Expression in the IDCP Region

Spatial gene expression analysis revealed upregulation of epithelial markers EPCAM and KRT8 across all clusters (Figure 2A), consistent with the findings from the violin plots (Figure 2B). Moreover, examination of gene expression and violin plots demonstrated high expression of a group of AR signature genes, including *KLK3*, *AR*, *TMPRSS2*, *NKX3.1*, and *AMACR* across all clusters (Figure 2C,D), indicating their tumor origin.

Furthermore, spatial gene expression analysis and violin plots showed the upregulation of *MUC6*, *MYO16*, *NPY*, and *KLK12* in the IDCP region, with expression diminishing as the distance from the IDCP region increased (Figure 2E,F). Additionally, gene expression analysis and violin plots revealed a relatively high expression of homologous recombination repair (HRR) genes, such as *CHEK2*, *TOP2A*, *TOP2B*, *PALB2*, and *SPOP*, in the IDCP region (Figure 3A,B). However, upregulation of *BRCA1* or *BRCA2* was not observed.

TMPRSS2, a known IDCP-associated gene, was highly expressed at the IDCP site without any evidence of *PTEN* downregulation (Figure 3C,D).

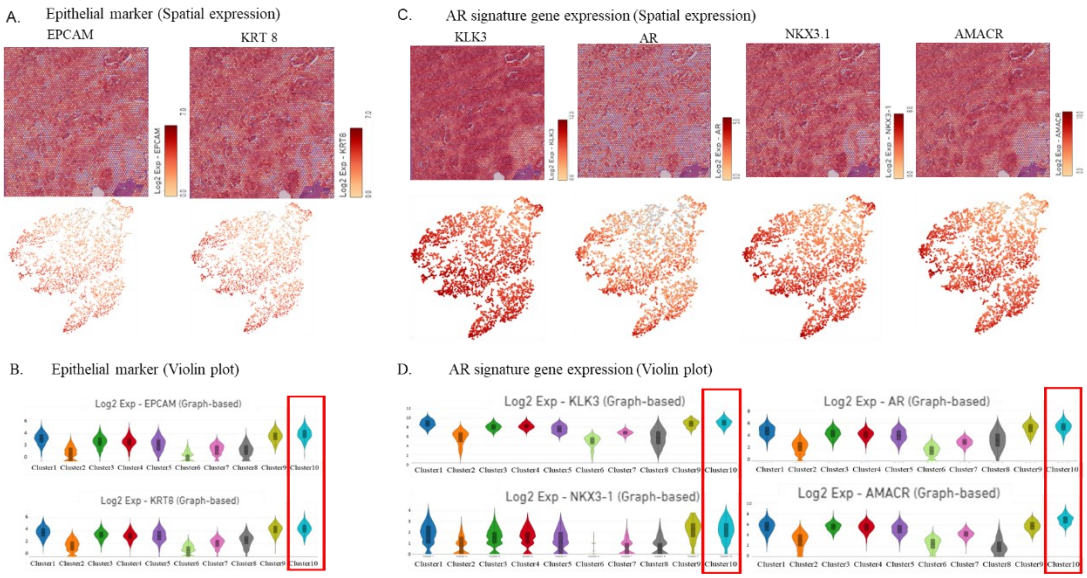

Figure 2. Visualization of the expression of epithelial marker genes, AR signature genes, and other upregulated genes in the IDCP region. (A, B) Spatial gene expression analysis showing that the epithelial markers were upregulated in all clusters (A), with similar findings in the violin plot (B). (C, D) Spatial gene expression analysis (C) and violin plot (D) showing the expression of a group of AR

 doi:10.20944/preprints202403.1037.v1

signature genes. (E, F) Spatial gene expression analysis (E) and violin plots (F) demonstrating the expression of MUC6, MYO16, NPY, and KLK12.

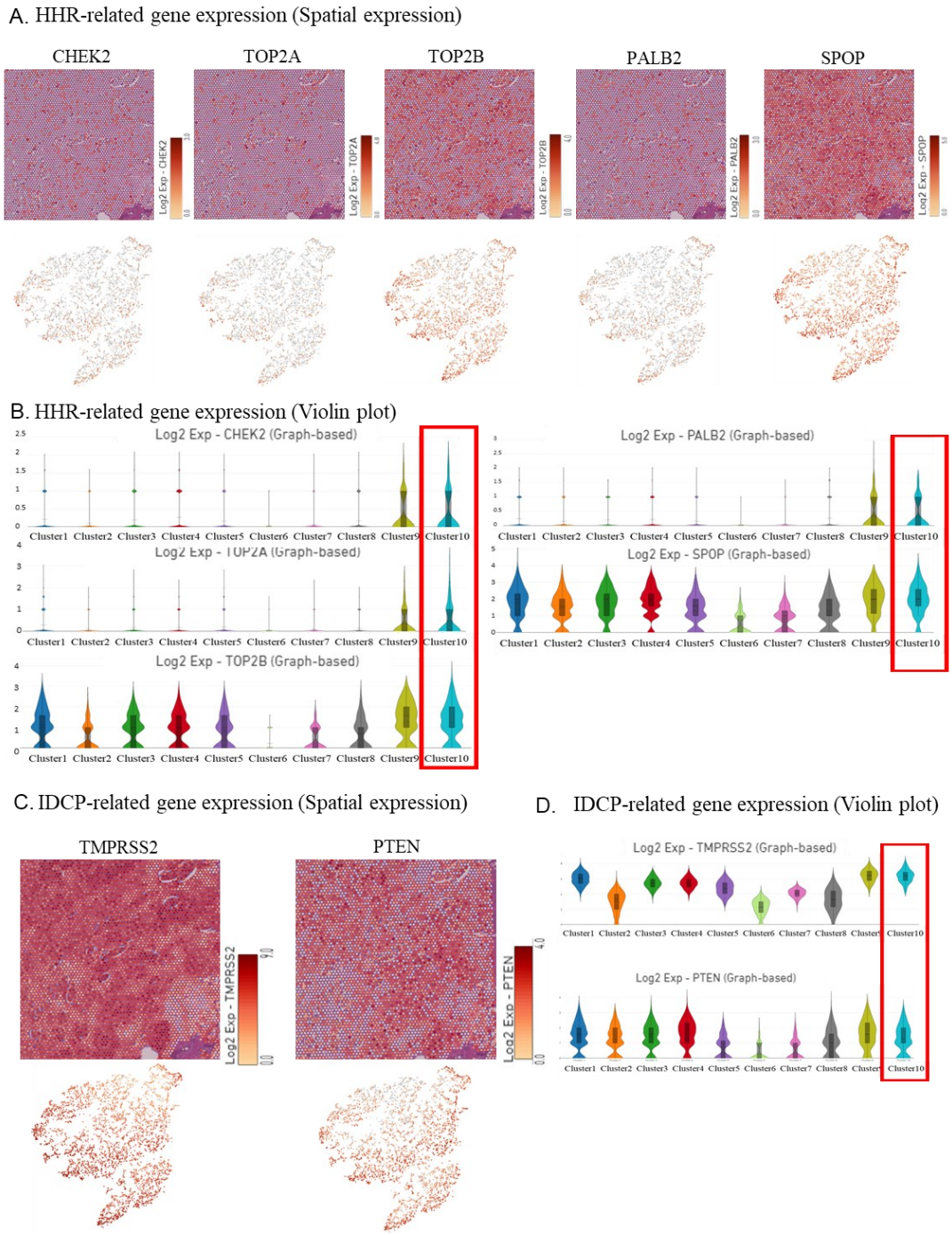

Figure 3. Visualization of the expression of HRR genes. (A, B) Spatial gene expression analysis (A) and violin plot (B) showing homologous recombination repair (HRR) gene expression. (C, D) Spatial gene expression analysis (C) and violin plot (D) showing TMPRSS2 and PTEN expression.

 doi:10.20944/preprints202403.1037.v1

3.3. Visualization of the Expression of IDCP Fibroblast Markers, Immune Cell Markers, and Hypoxia Markers

Spatial gene expression analysis and violin plots indicated downregulation of the fibroblast markers *COL1A2*, *DCN*, and *LUM* in the IDCP cluster (Figure 4A,B). Moreover, spatial gene expression analysis and violin plots demonstrated a low expression of the immune cell markers *CCL5*, *FCG3A*, and *TRAC* in the IDCP cluster (Figure 4C,D). Spatial gene expression analysis and violin plots revealed no significant differences in the epithelial cell markers between the clusters (Figure 4E,F). Additionally, analysis of the gene expression and violin plots revealed high expression of the hypoxia markers *HIF1A*, *BNIP3L*, *PDK1*, and *POGLUT1* in the IDCP cluster (Figure 4G,H). This suggested that the loss of immune cells and accumulation of hypoxic markers limited to the IDCP site may be attributed to the anatomic isolation of the IDCP site.

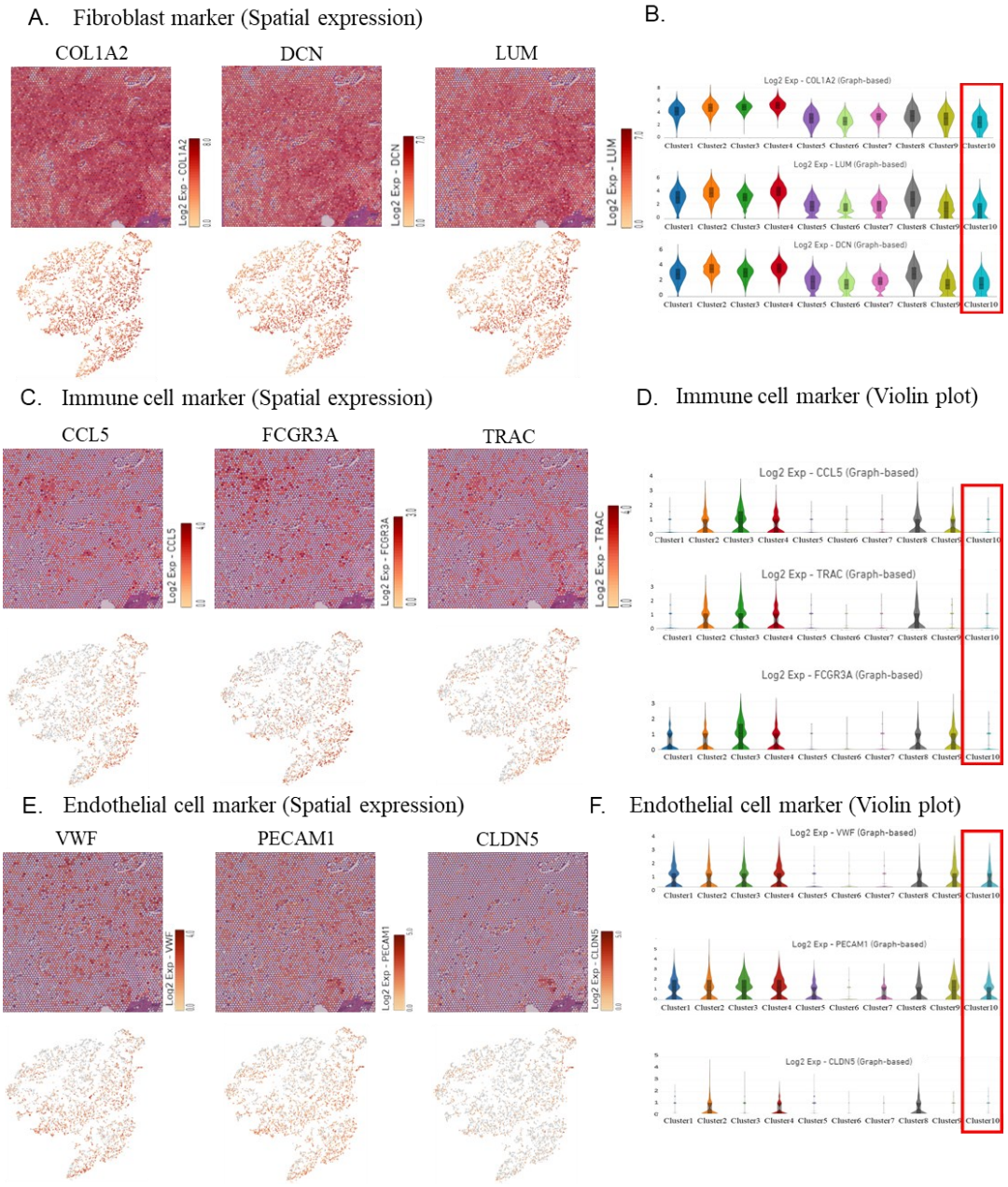

 doi:10.20944/preprints202403.1037.v1

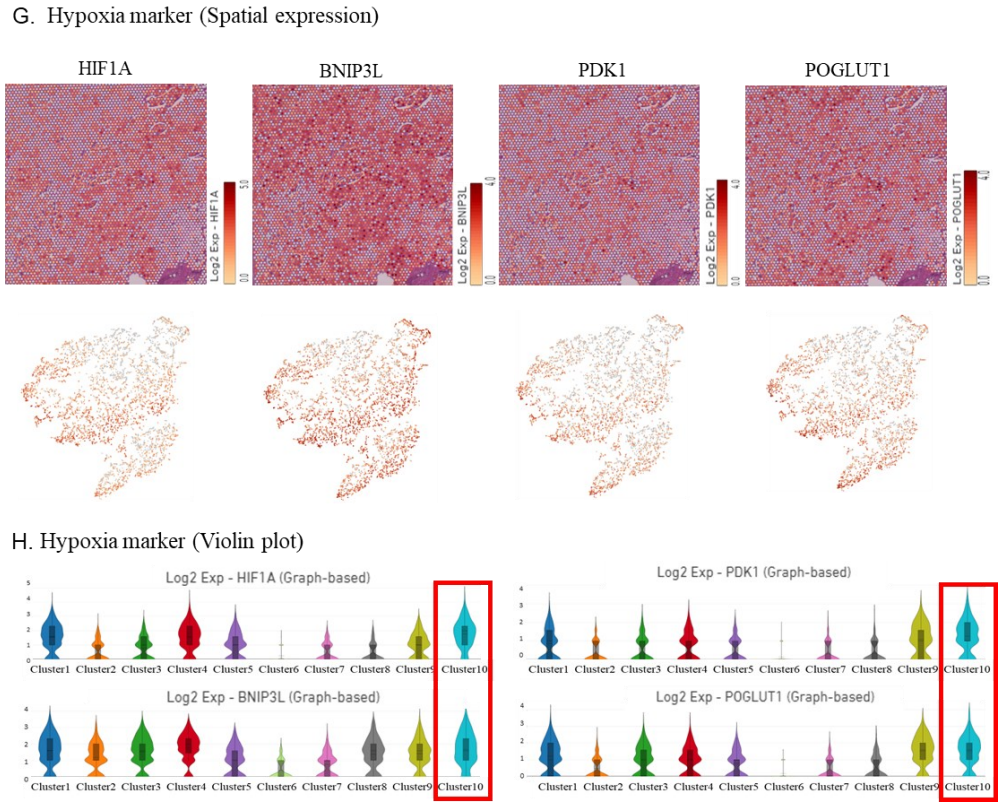

Figure 4. Visualization of the expression of fibroblast, immune cell, endothelial cell, and hypoxia markers. (A, B) Spatial gene expression analysis (A) and the violin plot (B) showing fibroblast marker gene expression. (C, D) Spatial gene expression analysis (C) and the violin plot (D) showing immune cell marker gene expression. (E, F) Spatial gene expression analysis (E) and the violin plot (F) showing endothelial cell marker gene expression. (G, H) Spatial gene expression analysis (G) and the violin plot (H) showing hypoxia marker gene expression.

4. Discussion

IDCP is a significant pathological finding with clinical prognostic implications. Haffner et al. conducted microdissection of both IDCP and surrounding invasive carcinoma sites and discerned site-specific gene expression patterns through their comparison. Consequently, they proposed a retrograde colony formation model wherein the *TMPRSS2-ERG* fusion gene-positive/*PTEN* loss component of invasive carcinoma infiltrates normal glandular ducts, forming IDCPs [2]. However, the precise sampling of lesion sites via microdissection is challenging and labor-intensive. Through single-cell analysis, Wong et al. compared cribriform carcinoma tissues with benign prostate tissues to elucidate the gene expression characteristics of cribriform prostate cancer [20]. Nonetheless, this study associated invasive cribriform carcinoma with IDCP but did not examine IDCP-specific gene abnormalities. Moreover, single-cell analyses lack spatial information, which impedes the identification of IDCP-derived cells. Therefore, we endeavored to identify IDCP-specific gene aberrations using spatial gene expression analysis.

An accurate diagnosis of IDCP is imperative for suitable treatment. IDCP has a significant prognostic value even in low-grade prostate cancer and should not be disregarded [21–23]. However, the classification of precursor-like (isolated) IDCP, a borderline lesion resembling HGPIN without a discernible cribriform pattern—remains contentious [24]. Therefore, in our study, we included samples from patients with a typical IDCP morphology, associated with high-grade prostate cancer. Following the IDCP diagnosis by two pathologists at our institution, the final diagnosis was confirmed by a pathologist in the United States who was experienced in diagnosing IDCP. The diagnosed case presented a typical IDCP morphology with surrounding invasive carcinoma,

 doi:10.20944/preprints202403.1037.v1

featuring a Gleason Score of 4+5 and a cribriform pattern tumor infiltrating the normal glandular ducts while retaining basal cells [25].

Spatial gene expression analysis revealed genetically similar tumors in and around the IDCP site. These tumors were *TMPRSS2*-positive but did not exhibit *PTEN* downregulation. As spatial gene expression analysis cannot identify mutations, potential *PTEN* mutations may have been overlooked. Nevertheless, genes upregulated at the IDCP site resembled those in clusters 1 and 5 adjacent to the IDCP. These findings support the hypothesis that the surrounding invasive carcinoma infiltrates normal glandular ducts. It is speculated that tumor cell clusters that have acquired high invasiveness form IDCP by invading and proliferating in normal glandular ducts with low tumor density.

MUC6, *MYO16*, *NPY*, and *KLK12* were upregulated at the IDCP site. *MUC6*, which encodes a member of the mucin protein family, is an organ specific antigen and plays a pivotal role in epithelial surface cryoprotection. Some literatures insists that *MUC16* serves as a tumor marker in gastric and other cancers [26,27]. Compared to other *KLK* genes, both *KLK6* and *KLK12* are associated with increased invasive potential [28,29]. *MYO16*, which encodes the myosin XVI protein, regulates neuronal morphogenesis [30]. In addition, *NPY* (neuropeptide Y), a member of the *NPY* family, is widely expressed in the central nervous system, and its receptor, *NPY-1R*, is associated with the proliferative potential of prostate cancer [31,32]. These results indicate that IDCP may be involved in prostate cancer neuroendocrine differentiation, although the NE signature markers *CHGA*, *SYP*, *NCAM1 (CD56)*, *NKX2.1*, *MYCN*, and *AURKA* were not elevated in the present case.

Heterozygous deletions of *PTEN*, *TP53*, and *RB1* are important genetic alterations associated with neuroendocrine prostate cancer (NEPC), and are frequently observed in IDCP, suggesting possible molecular similarities between NEPC and IDCP. In a limited case series, Ikeda et al. observed the components of IDCP in nine patients with NEPC for whom tissue specimens were available at diagnosis [33]. Thus, the identification of IDCP may serve as a potential predictor of NEPC development; however, the association between IDCP and NEPC remains unclear and warrants further investigation.

IDCP upregulates several homologous recombination repair (HRR) genes. In the present case, increased expression of *TOP2A*, *TOP2B*, and *SPOP* was observed. In a previous report, accumulation of *TOP2A* induced by *SPOP* mutations was found to facilitate prostate cancer progression through the accumulation of DNA damage, and etoposide was found effective against SPOP-mutated prostate cancer [35]. In the present case, *TOP2A* upregulation and SPOP expression suggested the possible efficacy of *TOP2A* inhibitors, *Chek2* and *Palb2* were mildly upregulated at IDCP sites, but no overall upregulation was observed, further, high expression of HRR gene abnormalities suggested the potential efficacy of PARP inhibitors.

The decreased expression of fibroblast markers *COL1A2*, *DCN*, and *LUM*, and immune cell markers *CCR5* and *FCGR3A* at the IDCP site probably reflects poor cellular access to the tumor microenvironment owing to the anatomic isolation of IDCP. Fibroblast marker genes associated with stromal fibrosis contribute to malignant transformation through the proliferation of cancer-associated fibroblasts (CAFs) in various cancers [36–39]. However, considering the recent findings regarding the presence of cancer-promoting and cancer-suppressing fibroblasts [40], decreased numbers of tumor-suppressing fibroblasts and immune cells in the IDCP region may contribute to malignant transformation. Furthermore, the elimination of immune cells from the inherently "immune-cold" tumor microenvironment of prostate cancer may render immune checkpoint inhibitors ineffective [41]. Furthermore, IDCP sites exhibited increased levels of hypoxia markers such as *HIF1A*, *BNIP3L*, *PDK1*, and *POGLUT1*. IDCPs growing within narrowly isolated normal glandular ducts are susceptible to hypoxia, which induces tumor cell starvation and hypoxic stress, increases glycolytic metabolism and angiogenesis, and increases the potential for metastasis and invasion. Thus, IDCP may promote malignant transformation and resistance to therapy by inducing hypoxia and inaccessibility of immune cells owing to its morphological features (Figure 5). Focusing on the hypoxic state of IDCP, patients with prostate cancer and IDCP may benefit from inhibitors targeting *HIF1A*. In the present study, no increase in endothelial cell marker levels was observed despite the

 doi:10.20944/preprints202403.1037.v1

presence of hypoxia at the IDCP site. This implies that IDCP is an isolated and anomalous lesion, in which angiogenesis is less likely to be induced.

As this was a comparative analysis between IDCP and tumor sites with similar gene expression levels, identifying dramatic differences in gene expression was difficult. However, this study clearly demonstrated that IDCP can be recognized as a distinct cluster that tends to show the characteristic expression of markers related to immune cells, fibroblasts, and hypoxia. Because this was a single case study, the need to examine more cases in the future is acknowledged. As spatial gene expression analysis is dot-based, each dot contains the gene expression of approximately 10 cells. In fact, all 10 clusters of tumor cells classified in this study contained a mixture of immune cell and fibroblast markers. Integrating single-cell analysis data using the same sample through bioinformatics and introducing high-resolution spatial gene expression analysis at the single-cell level is thus necessary to perform a more accurate analysis. This will allow for a more accurate analysis.

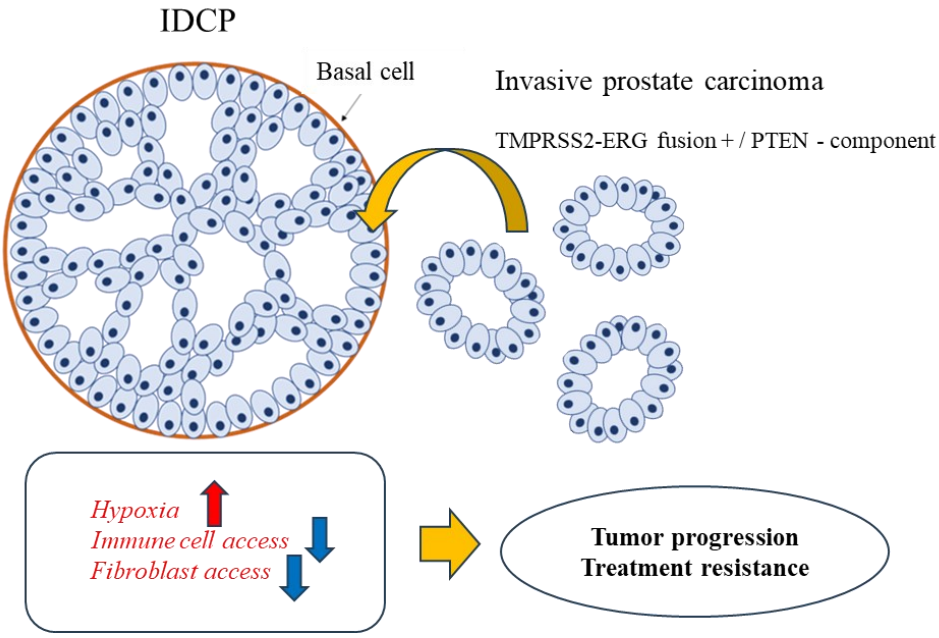

Figure 5. Graphical Summary. Intraductal carcinoma of the prostate may promote malignant transformation and increase resistance to therapy by causing hypoxia and immune cell inaccessibility owing to its morphological features.

5. Conclusion

Spatial gene expression analysis could identify IDCP-specific gene expression profiles effectively in a typical IDCP case. Our findings suggest that the morphological features of IDCP contribute to its poor accessibility for fibroblasts and immune cells, potentially playing a role in malignant transformation and therapeutic resistance. Overall, this study elucidates valuable markers and malignant mechanisms for diagnosing prostate cancer cases with IDCP, and provides novel personalized treatment options. Moving forward, we aim to further elucidate these mechanisms by expanding our sample size, integrating our data with single-cell analysis data, and implementing high-resolution spatial gene expression analysis techniques.

Author Contributions: For All authors have read and approved the manuscript. R W and T S: Project development, Data analysis, Manuscript writing/editing; N M and T K: Project development, Data analysis; M K and R K: Data collection.

Funding: This research was funded by JSPS KAKENHI (Grant Number 22K09449). Medical Research Grants of Takeda Science Foundation. Japanese Foundation for Prostate Research. Japanese Urological Association Young Research Grant. Takahashi Industrial and Economic Research Foundation

Institutional Review Board Statement: This study was approved by the Institutional Review Board of Ehime University (No. 2205001) and conducted according to the principles of the Declaration of Helsinki.

Informed Consent Statement: Written informed consent was obtained from all participants to publish the original article and accompanying images.

Data Availability Statement: The data supporting the findings of this study are available from the corresponding author upon reasonable request. Data Availability Statement: The raw and processed data of spatial transcriptomics generated in this study are openly available in GEO at https://www.ncbi.nlm.nih.gov/geo/, GEO number {GSE230282}.

Acknowledgments: We express our sincere thanks to Dr. Michael Haffner at Fred Hutchinson Cancer Center for advising on IDCP diagnosis; to Dr. Daisuke Motooka at the Research Institute for Microbial Diseases (RIMD) at Osaka University for supporting the sequence of CytAssist Visium; and to Dr. Tony LH Chu of the Human Biology division, Fred Hutchinson Cancer Center, for his support in the data analysis. This work was supported by JSPS KAKENHI (Grant Number 22K09449), Medical Research Grants of Takeda Science Foundation, Japanese Foundation for Prostate Research and Japanese Urological Association Young Research Grant

Conflicts of Interest: The authors declare no conflicts of interest.

References

1. McNeal JE, Yemoto CE. Spread of adenocarcinoma within prostatic ducts and acini. Morphologic and clinical correlations. Am J Surg Pathol. 1996 Jul;20(7):802-14. https://doi.org/10.1097/00000478-199607000-00003.
2. Haffner MC, Weier C, Xu MM, Vaghasia A, Gürel B, Gümüşkaya B et al. Molecular evidence that invasive adenocarcinoma can mimic prostatic intraepithelial neoplasia (PIN) and intraductal carcinoma through retrograde glandular colonization. J. Pathol. 2016; 238: 31–41. https://doi.org/10.1002/path.4628.
3. Tsuzuki T. Intraductal carcinoma of the prostate: a comprehensive and updated review. Int. J. Urol. 2015; 22: 140–5. https://doi.org/10.1111/iju.12657.
4. Zhou M. Intraductal carcinoma of the prostate: the whole story. Pathology. 2013; 45: 533–9. https://doi.org/10.1097/PAT.0b013e3283653322.
5. Varma M, Delahunt B, Egevad L, Samaratunga H, Kristiansen G. Intraductal carcinoma of the prostate: A critical re-appraisal. Virchows Arch. 2019; 474: 525–34. https://doi.org/10.1007/s00428-019-02544-6.
6. Miura N, Mori K, Mostafaei H, Quhal F, Motlagh RS, Pradere B et al. The prognostic impact of intraductal carcinoma of the prostate: A systematic review and meta-analysis. J. Urol. 2020; 204: 909–17. https://doi.org/10.1097/JU.0000000000001290.
7. Kimura K, Tsuzuki T, Kato M, Saito AM, Sassa N, Ishida R, Hirabayashi H, Yoshino Y, Hattori R, Gotoh M. Prognostic value of intraductal carcinoma of the prostate in radical prostatectomy specimens. Prostate. 2014 May;74(6):680-7. https://doi.org/10.1002/pros.22786. Epub 2014 Jan 31.
8. Zhao T, Liao B, Yao J, Liu J, Huang R, Shen P, Peng Z, et al. Is there any prognostic impact of intraductal carcinoma of prostate in initial diagnosed aggressively metastatic prostate cancer? Prostate. 2015 Feb 15;75(3):225-32. https://doi.org/10.1002/pros.22906. Epub 2014 Oct 13.
9. Kato M, Tsuzuki T, Kimura K, Hirakawa A, Kinoshita F, Sassa N, Ishida R et al. The presence of intraductal carcinoma of the prostate in needle biopsy is a significant prognostic factor for prostate cancer patients with distant metastasis at initial presentation. Mod Pathol. 2016 Feb;29(2):166-73. https://doi.org/10.1038/modpathol.2015.146. Epub 2016 Jan 8.
10. Epstein JI, Egevad L, Amin MB, Delahunt B, Srigley JR, Humphrey PA The 2014 International Society of Urological Pathology (ISUP) Consensus Conference on Gleason Grading of Prostatic Carcinoma: Definition of Grading Patterns and Proposal for a New Grading System. Am. J. Surg. Pathol. 2016; 40: 244–52. https://doi.org/10.1097/PAS.0000000000000530.
11. Humphrey PA, Moch H, Cubilla AL, Ulbright TM, Reuter VE. The 2016 WHO classification of tumours of the urinary system and male Genital Organs-Part B: prostate and bladder tumours. Eur. Urol. 2016; 70: 106–19. https://doi.org/10.1016/j.eururo.2016.02.028.
12. Network NCC NCCN clinical practice guidelines in oncology: prostate cancer, version 1. 2023.
13. Han B, Suleman K, Wang L, Siddiqui J, Sercia L, Magi-Galluzzi C et al. ETS gene aberrations in atypical cribriform lesions of the prostate: implications for the distinction between intraductal carcinoma of the prostate and cribriform high-grade prostatic intraepithelial neoplasia. Am J. Surg. Pathol. 2010; 34: 478–85. https://doi.org/10.1097/PAS.0b013e3181d6827b.
14. Bettendorf O, Schmidt H, Staebler A, Grobholz R, Heinecke A, Boecker W et al. Chromosomal imbalances, loss of heterozygosity, and immunohistochemical expression of TP53, RB1, and PTEN in intraductal cancer, intraepithelial neoplasia, and invasive adenocarcinoma of the prostate. Genes Chromosom. Cancer. 2008; 47: 565–72. https://doi.org/10.1002/gcc.20560.
15. Wang Z, Wang Y, Zhang J, Hu Q, Zhi F, Zhang S, Mao D et al. Significance of the TMPRSS2:ERG gene fusion in prostate cancer. Mol. Med. Rep. 2017; 16: 5450–58. https://doi.org/10.3892/mmr.2017.7281.

16. Shah RB, Shore KT, Yoon J, Mendrinos S, McKenney JK, Tian W. PTEN loss in prostatic adenocarcinoma correlates with specific adverse histologic features (intraductal carcinoma, cribriform Gleason pattern 4 and stromogenic carcinoma). Prostate. 2019; 79: 1267–73. https://doi.org/10.1002/pros.23831.
17. Risbridger GP, Taylor RA, Clouston D, Sliwinski A, Thorne H, Hunter S et al. Patient-derived xenografts reveal that intraductal carcinoma of the prostate is a prominent pathology in BRCA2 mutation carriers with prostate cancer and correlates with poor prognosis. Eur. Urol. 2015; 67: 496–503. https://doi.org/10.1016/j.eururo.2014.08.007.
18. Taylor RA, Fraser M, Rebello RJ, Boutros PC, Murphy DG, Bristow RG, Risbridger GP. The influence of BRCA2 mutation on localized prostate cancer. Nat. Rev. Urol. 2019; 16: 281–90. https://doi.org/10.1038/s41585-019-0164-8.
19. Watanabe R, Miura N, Kurata M, Kitazawa R, Kikugawa T, Saika T. Spatial Gene Expression Analysis Reveals Characteristic Gene Expression Patterns of De Novo Neuroendocrine Prostate Cancer Coexisting with Androgen Receptor Pathway Prostate Cancer. Int J Mol Sci. 2023 May 18;24(10):8955. https://doi.org/10.3390/ijms24108955.
20. Wong HY, Sheng Q, Hesterberg AB, Croessmann S, Rios BL, Giri K, Jackson J et al. Single cell analysis of cribriform prostate cancer reveals cell intrinsic and tumor microenvironmental pathways of aggressive disease. Nat Commun. 2022 Oct 13;13(1):6036. https://doi.org/10.1038/s41467-022-33780-1.
21. Miyai K, Divatia MK, Shen SS, Miles BJ, Ayala AG, Ro JY. Heterogeneous clinicopathological features of intraductal carcinoma of the prostate: a comparison between "precursor-like" and "regular type" lesions. Int J Clin Exp Pathol. 2014 Apr 15;7(5):2518-26. eCollection 2014.
22. Guo CC, Epstein JI. Intraductal carcinoma of the prostate on needle biopsy: Histologic features and clinical significance. Mod Pathol. 2006 Dec;19(12):1528-35. https://doi.org/10.1038/modpathol.3800702. Epub 2006 Sep 15.
23. Robinson BD, Epstein JI. Intraductal carcinoma of the prostate without invasive carcinoma on needle biopsy: emphasis on radical prostatectomy findings. J Urol. 2010 Oct;184(4):1328-33. https://doi.org/10.1016/j.juro.2010.06.017. Epub 2010 Aug 17.
24. Varma M, Epstein JI. Head to head: should the intraductal component of invasive prostate cancer be graded? Histopathology. 2021; 78: 231–39. https://doi.org/10.1111/his.14216.
25. Zong Y, Montironi R, Massari F, Jiang Z, Lopez-Beltran A, Wheeler TM et al. Intraductal carcinoma of the prostate: pathogenesis and molecular perspectives. Eur. Urol. Focus. 2021; 7: 955–63. https://doi.org/10.1016/j.euf.2020.10.007.
26. Fulgione C, Raffone A, Travaglino A, Arciuolo D, Santoro A, Cianfrini F, Russo D et al. Diagnostic accuracy of HIK1083 and MUC6 as immunohistochemical markers of endocervical gastric-type adenocarcinoma: A systematic review and meta-analysis. Pathol Res Pract. 2023 Jan;241:154261. https://doi.org/10.1016/j.prp.2022.154261. Epub 2022 Dec 5.
27. Yamanoi K, Fujii C, Yuzuriha H, Kumazawa M, Shimoda M, Emoto K, Asamura H, Nakayama J. MUC6 expression is a preferable prognostic marker for invasive mucinous adenocarcinoma of the lung. Histochem Cell Biol. 2022 Jun;157(6):671-684. https://doi.org/10.1007/s00418-022-02093-1. Epub 2022 Mar 30.
28. Lose, F.; Batra, J.; O'Mara, T.; Fahey, P.; Marquart, L.; Eeles, R.A.; et al. Common Variation in Kallikrein Genes KLK5, KLK6, KLK12, and KLK13 and Risk of Prostate Cancer and Tumor Aggressiveness. Urol. Oncol. 2013, 31, 635-643. https://doi.org/10.1016/j.urolonc.2011.05.011.
29. Korbakis, D.; Soosaipillai, A.; Diamandis, E.P. Study of Kallikrein-related Peptidase 6 (KLK6) and Its Complex with α1-Antitrypsin in Biological Fluids. Clin. Chem. Lab. Med. 2017, 55, 1385-1396. https://doi.org/10.1515/cclm-2017-0017.
30. Yamanoi K, Fujii C, Yuzuriha H, Kumazawa M, Shimoda M, Emoto K, Asamura H, Nakayama J. MUC6 expression is a preferable prognostic marker for invasive mucinous adenocarcinoma of the lung. Histochem Cell Biol. 2022 Jun;157(6):671-684. https://doi.org/10.1007/s00418-022-02093-1. Epub 2022 Mar 30.
31. Massimiliano Ruscica, Elena Dozio, Stéphane Boghossian, Giorgio Bovo, Vera Martos Riaño, Marcella Motta, Paolo Magni. Activation of the Y1 receptor by neuropeptide Y regulates the growth of prostate cancer cells. Endocrinology. 2006 Mar;147(3):1466-73. https://doi.org/10.1210/en.2005-0925. Epub 2005 Dec 8.
32. Sigorski D, Wesołowski W, Gruszecka A, Gulczyński J, Zieliński P, Misiukiewicz S, Kitlińska J, Iżycka-Świeszewska E. Neuropeptide Y and its receptors in prostate cancer: associations with cancer invasiveness and perineural spread. J Cancer Res Clin Oncol. 2023 Aug;149(9):5803-5822. https://doi.org/10.1007/s00432-022-04540-x. Epub 2022 Dec 30.
33. Ikeda J, Ohe C, Ohsugi H, Matsuda T, Tsuta K, Kinoshita H. Association of intraductal carcinoma of the prostate detected by initial histological specimen and neuroendocrine prostate cancer: A report of three cases. Pathol Int. 2021 Sep;71(9):621-626. https://doi.org/10.1111/pin.13137 . Epub 2021 Jul 23.

34. Naito Y, Kato M, Nagayama J, Sano Y, Matsuo K, Inoue S, Sano T et al. Recent insights on the clinical, pathological, and molecular features of intraductal carcinoma of the prostate. Int J Urol. 2024 Jan;31(1):7-16. https://doi.org/10.1111/iju.15299. Epub 2023 Sep 20.
35. Watanabe R, Maekawa M, Hieda M, Taguchi T, Miura N, Kikugawa T, Saika T, Higashiyama S. S POP is essential for DNA-protein cross-link repair in prostate cancer cells: SPOP-dependent removal of topoisomerase 2A from the topoisomerase 2A-DNA cleavage complex. Mol Biol Cell. 2020 Mar 15;31(6):478-490. https://doi.org/10.1091/mbc.E19-08-0456. Epub 2020 Jan 22.
36. Luu Hoang, K.N.; Anstee, J.E.; Arnold, J.N. The Diverse Roles of Heme Oxygenase-1 in Tumor Progression. Front. Immunol. 2021, 12, 658315. https://doi.org/10.3389/fimmu.2021.658315.
37. Liu, T.; Zhou, L.; Li, D.; Andl, T.; Zhang, Y. Cancer-associated Fibroblasts Build and Secure the Tumor Microenvi-ronment. Front. Cell Dev. Biol. 2019, 7, 60. https://doi.org/10.3389/fcell.2019.00060.
38. Ren, J.; Smid, M.; Iaria, J.; Salvatori, D.C.F.; van Dam, H.; Zhu, H.J.; et al. Cancer-associated Fibroblast-derived Gremlin 1 Promotes Breast Cancer Progression. Breast Cancer Res. 2019, 21, 109. https://doi.org/10.1186/s13058-019-1194-0.
39. de Hosson, L.D.; Takkenkamp, T.J.; Kats-Ugurlu, G.; Bouma, G.; Bulthuis, M.; de Vries, E.G.E.; et al. Neuroendocrine Tumours and Their Microenvironment. Cancer Immunol. Immunother. 2020, 69, 1449-1459. https://doi.org/10.1007/s00262-020-02556-1.
40. Kobayashi H, Enomoto A, Woods SL, Burt AD, Takahashi M, Worthley DL. Cancer-associated fibroblasts in gastrointestinal cancer. Nat Rev Gastroenterol Hepatol. 2019 May;16(5):282-295. https://doi.org/10.1038/s41575-019-0115-0.
41. Séguier D, Adams ES, Kotamarti S, D'Anniballe V, Michael ZD, Deivasigamani S, Olivier J et al. Intratumoural immunotherapy plus focal thermal ablation for localized prostate cancer. Nat Rev Urol. 2023 Dec 19. https://doi.org/10.1038/s41585-023-00834-y.